ACS Sustainable Chemistry & Engineering

pubs.acs.org/journal/ascecg

Research Article

Understanding H_2O_2-Induced Thermo-Oxidative Reclamation of Vulcanized Styrene Butadiene Rubber at Low Temperatures

Zhen Zhang, Jiayi Li, Chaoying Wan, Yuxin Zhang, and Shifeng Wang*

Cite This: https://dx.doi.org/10.1021/acssuschemeng.0c08867

Read Online

ACCESS | Metrics & More | Article Recommendations | Supporting Information

ABSTRACT: Recombination reactions often occur in the process of chemical, thermal, or mechanical degradation of vulcanized styrene butadiene rubber (SBR), which hinders the recycling efficiency of waste tire rubbers. In this work, we developed an effective method to transform solid vulcanized SBR into reclaimed rubber with 100% sol fraction through a hydrogen peroxide (H_2O_2)-induced thermo-oxidative reclamation process at 100 °C with the assistance of soybean oil. The structural evolution of the vulcanized SBR and the role of H_2O_2 and soybean oil in the reclaiming process were investigated by sol−gel analysis, gel permeation chromatography (GPC), attenuated total reflectance−Fourier transform infrared spectroscopy (ATR−FTIR), and ^{13}C nuclear magnetic resonance (^{13}C NMR) spectroscopy. The results showed that vulcanized SBR underwent severe oxidative scission, the sol of the reclaimed samples increased from 20.4 wt % up to 100 wt % with a decreased molecular weight to 1.378×10^4 g/mol. Multiple functional groups such as carboxyl, hydroxyl, and ether groups were generated in the polymer chains as confirmed by ^{13}C NMR and FTIR spectroscopy. Moreover, the reaction pathway of the oxidative reclamation was quantified by density functional theory (DFT) calculations, suggesting that hydroxyl radicals were generated from a homolytic cleavage reaction of H_2O_2 with SBR by hydrogen abstraction and accelerated the rate-determining step of the SBR oxidation. The apparent activation energy (E_a) of the initial stage of the oxidative reclamation decreased from 223 to 160 kJ/mol according to the model-free kinetics results.



KEYWORDS: *styrene butadiene rubber, oxidative reclamation, hydrogen peroxide, reclaimed rubber*

Downloaded via SHANGHAI JIAO TONG UNIV on January 25, 2021 at 05:59:50 (UTC).
See https://pubs.acs.org/sharingguidelines for options on how to legitimately share published articles.

INTRODUCTION

The rapid development of automotive industry consumes large amounts of tires annually, resulting in substantial waste tire rubber worldwide, and the number of waste tires is estimated to be 1200 million by 2030.[1,2] These waste tire rubbers are not reprocessable and reusable because of the permanent covalent cross-linked polymer networks; therefore, most waste rubber is still treated in landfill or incineration, which causes serious environmental pollution and eco-toxicity.[3,4] How to effectively recycle and reuse waste tire rubber has become an increasingly important topic for both academia and industry.

Recycling methods such as grinding, reclaiming, or pyrolysis have been developed to reprocess the problematic waste rubber.[5−8] Among which, reclaiming is of growing importance from the view of high cost of raw materials, nonrenewable fossil fuels, and environmental sustainability.[9,10] The reclaimed rubber often contains large amounts of residual cross-linked structures, which causes poor processability and weak interfacial adhesion when compounded with raw rubber.[11,12] The poor interfacial adhesion negatively affects the mechanical performance of the rubber blends and thus limits the applications of reclaimed rubber. Therefore, an effective treatment method is needed to break the covalent cross-linked network of waste tire rubber in order to improve the reprocessability.

Waste tire rubber is a complex composite containing natural rubber (NR, ∼45 wt %), SBR (∼20 wt %), carbon black (25−35 wt %), and other organic components, such as zinc oxide and sulfur. Reclamation of natural rubber (NR) has made great progress so far, thanks to its intrinsic "poor molecular integrity" of the polyisoprene polymer chain.[13] The reclaiming of SBR is still challenging because of its re-crosslinking reaction.[14,15] A recent study showed that by adding diphenyl disulfide (DPDS) and distillate aromatic extract oil, only 16 wt % sol fraction of vulcanized SBR was obtained at 220 °C, while the NR polymer network was nearly completely destructed.[16] Isayev et al. conducted ultrasonication treatment to assist SBR reclamation but it resulted in an increased crosslink density of SBR.[17−20]

Received: December 6, 2020
Revised: January 8, 2021

© XXXX American Chemical Society

These results demonstrated that the reclamation of vulcanized SBR was accompanied by a re-crosslinking reaction because of the presence of highly reactive allylic radicals during the reclamation process.[21,22] These active radicals can be quenched by adding small molecule chemicals, such as DPDS, di(2-aminophenyl) disulfide (APDS), and oxidation stabilizers (Irganox 1076). The reversion phenomenon was reduced, and the reclamation of vulcanized SBR was well controlled at above 220 °C.[23] However, this process was conducted with the introduction of sulfur-containing chemicals at a relatively high temperature, associated with the emission of hazardous gas. So far, a green and effective reclamation of vulcanized SBR is yet to be explored.

Unsaturated rubber materials can be thermally oxidated for decrosslinking. During the thermo-oxidation process of vulcanized SBR, re-crosslinking reactions occur because of the recombination among macroradicals, thus leading to a low sol fraction.[16] In our previous work, vulcanized SBR blended with soybean oil was degraded by thermo-oxidation at 150 °C, resulting in 47.3 wt % sol fraction.[24] Compared with the sol fraction of reclaimed NR samples, the reclamation efficiency of SBR still needs to be improved. The introduction of highly active free radicals is an effective solution to suppress the re-crosslinking reaction by quenching the radicals.

Hydrogen peroxide (H_2O_2) is a strong oxidizing agent and can quickly decompose into hydroxyl radicals ($^{\bullet}OH$) at low temperatures.[25,26] The $^{\bullet}OH$ are highly reactive, which can lead to hydrogen atom abstraction of rubber chains and quench the allylic radicals. Ibrahim et al. reported that by using H_2O_2 and $NaNO_2$ as the reagents, high molecular weight NR was transformed into liquid NR at 70 °C.[27] H_2O_2 thus has a potential as both an initiator and radical stabilizer for rubber oxidation at low temperature. However, H_2O_2 has poor compatibility with covalent cross-linked rubber networks. To address this issue, soybean oil can be used to effectively swell the rubber matrix and facilitate the penetration of H_2O_2 into the rubber structures.

In this work, we report a low-temperature process for effectively reclaiming vulcanized SBR in the presence of H_2O_2. This reclaiming process avoids the use of sulfur-containing chemical agents and high temperature, reducing the release of toxic gases. The structural evolution of the reclaimed samples was examined based on sol−gel analysis and Horikx theory. Chemical changes of the reclaimed samples were investigated using attenuated total reflectance-Fourier transform infrared spectroscopy (ATR−FTIR), ^{13}C nuclear magnetic resonance (^{13}C NMR) spectroscopy, and gel permeation chromatography (GPC). Moreover, the reclamation mechanism was studied by density functional theory (DFT) calculations and model-free kinetics analysis.

EXPERIMENTAL SECTION

Materials. SBR1502 with styrene of 22.5−24.5% was purchased from Sinopec Qilu Petrochemical Company, China. Soybean oil was obtained from Shanghai Liangyou Oil Industry Co., Ltd. The vulcanizing agent (sulfur) and the accelerator (*N*-cyclohexyl-2-benzothiazolesulfenamide) as well as other additives such as stearic acid and zinc oxide are of commercial grade. Hydrogen peroxide (H_2O_2) (3 wt %) was obtained from Shanghai Lingfeng Chemical Reagent Co., Ltd. The solvent (toluene, acetone) was obtained from Sinopharm Group, China.

Preparation of Vulcanized SBR. Vulcanized SBR was prepared following the formulation: SBR 100 phr, sulfur 1.9 phr, zinc oxide 5 phr, stearic acid 2 phr, and *N*-cyclohexyl-2-benzothiazolesulfenamide (CZ) 1.6 phr.[24] Here, the "phr" stands for per hundred of rubber. The curing conditions were referred to from our previous work.[24]

Reclamation Process of Vulcanized SBR. The vulcanized SBR was masticated first for 10 min and then screened by a 10-mesh sieve to obtain the vulcanized SBR powders. The vulcanized SBR powders, soybean oil, and H_2O_2 were blended at different ratios. The mixed samples were stirred at 25 °C for 2 h to maximize swelling. Subsequently, the mixed samples (3.0 g) were moved into a drying oven (XMTD-8222, Jinghong Laboratory Instrument, Shanghai) at the designed temperature for 4 h with air supply (0.25 m^3/s). The reclaimed samples of vulcanized SBR were labeled as RH_2SBR_{100}, which contains 100 phr of soybean oil and 2 phr of H_2O_2. RH_2SBR_{200}-0.5 means that the sample is under oxidative reclamation for 0.5 h.

Characterization of Reclaimed Samples. The compositions and chemical structures of the reclaimed samples were characterized by the following methods. The models and producers of test instruments are shown in Table S3 (see Supporting Information) and also included below.

Soybean oil and rubber additives were removed from the samples (RH_2SBRs) using acetone. The sol fractions of RH_2SBRs (3.0 g) were separated using the Soxhlet extractor (Shanghai Heqi Glassware Co., Ltd, China). The detailed procedures of the extraction process were referred to our previous work.[24] The sol fraction was calculated by eq 1

$$S_f = \frac{m_0 - (m_1 + m_2)}{m_0 \times w} \times 100 \quad (1)$$

where S_f is the sol of the reclaimed samples, m_0 stands for the weight of the samples before treatment, and m_1 stands for the weight of the treated samples after extraction. m_2 is the weight of the samples extracted by acetone. w stands for the content of rubber.

After soybean oil was removed from the reclaimed samples, the samples were made into sheets. The sheets (~5.0 g) were placed in toluene to swell at 25 °C for three days. Subsequently, toluene on the surface of the samples was wiped off by using absorption paper, and the mass of the swollen samples were weighed. The crosslink density of the RHSBRs were solved by the Flory−Rehner formula, as shown in eqs 2 and 3

$$V_e = \frac{V_r + \chi V_r^2 + \ln(1 - V_r)}{V_s(0.5V_r - V_r^{1/3})} \quad (2)$$

$$V_r = \frac{m_r}{m_r + m_s(\rho_r/\rho_s)} \quad (3)$$

where V_e represents the crosslink density (mol/cm^3) and V_r stands for the volume percent of RHSBRs in the gel of the samples. V_s represents the molar volume of toluene (106.4 cm^3/mol), χ represents the Flory−Huggins polymer−solvent interaction parameter (0.43 for the SBR/toluene), m_r represents the weight of RHSBRs, m_s represents the weight of the solvent in the samples, ρ_r represents the density of RHSBRs, and ρ_s represents the density of the solvent toluene (0.867 g/cm^3).

The samples were heated from 50 to 700 °C by a thermo-gravimetric analyzer (TGA, Discovery TGA550, TA Instruments, USA) in an air atmosphere. The heating rates were set as 10, 20, 30, and 40 °C/min. The air gas flow rate was set as 60 mL/min.

The structures of SBR samples were investigated by ATR-FTIR (Spectrum 100, PerkinElmer, Inc., USA). The wavenumber region was set from 4000 to 650 cm^{-1}.

Molecular weight of the sol was measured using GPC (HLC-8320GPC, Tosoh Co., Japan). Tetrahydrofuran (flow rate: 0.35 mL/min) was used as the solvent.

Carbon-13 nuclear magnetic resonance (^{13}C NMR, AVANCE III HD 400, Bruker, Germany) was used to confirm the structure of the reclaimed SBR samples. The rubber samples were dissolved in $CDCl_3$ at 25 °C, and the spectra were obtained by an ADVANCE Bruker 400 MHz spectrometer.

The kinetic parameters of various chemical reactions are calculated by kinetic analysis. The activation energy (E_a) reflects the reaction energy dependent on the reaction routines and mechanism.[28] It can be calculated by both model-fitting (e.g., the Coats−Redfern method) and

https://dx.doi.org/10.1021/acssuschemeng.0c08867
ACS Sustainable Chem. Eng. XXXX, XXX, XXX−XXX

model-free (e.g., the Flynn−Wall−Ozawa method) methods.[29] The model-fitting methods require the preassumption of the reaction kinetic mechanism function and is derived from the assumption of constant activation energy processes. Therefore, it may cause significant errors involved in the activation energy. The model-free methods allow the E_a to be solved with no assumption of the reaction mechanism and can process varied activation energy processes.[30] Therefore, the Flynn−Wall−Ozawa method, one of the most widely used model-free methods, is used for determining the E_a for vulcanized SBR in this study. With proper assumptions and restrictions, the equation of the Flynn−Wall−Ozawa model-free method for the calculation of the E_a can be obtained from eq 4

$$\log_{10}\beta = \log_{10}\left[\frac{AR}{EG(\alpha)}\right] - 2.315 - 0.4567\frac{E}{RT} \quad (4)$$

where $G(\alpha)$ stands for the integration form of the reaction model, R represents the gas constant, A represents the pre-exponential factor, T stands for the absolute temperature in Kelvin, and β represents the heating rate of the process. The E_a at a certain conversion can be solved from the slope of $\log_{10}\beta \sim 1/T$. The model-free methods avoid the assumption of specific kinetic model and apply three or more sets of weight loss rates to solve the E_a of every conversion according to isoconversional methods.

Theoretical Calculation Method. Structural optimizations were performed with the M06-2X functional[31] and the 6-311G (d, p) level using Gaussian 16 (A.03) program package.[32] Their vibrational frequencies performed at the same level were performed to confirm each stationary point to be either an intermediate or a transition structure. Furthermore, the intrinsic reaction coordinates calculations were performed to identify transition states (TSs), reactants, and products. Then, the electronic energies and relative energies of molecules during the reaction were updated with the single point calculation using larger basis sets, that is M06-2X/def2-TZVP. The Fukui function was used to predict reactive sites at the M06-2X/6-311+G(d, p) level of theory in the Multiwfn 3.7 software package.[33] Fukui function is defined in eq 5[34,35]

$$f(r) = \left[\frac{\partial\rho(r)}{\partial N}\right]_v \quad (5)$$

In the formula, N represent number of electrons in the present system. For a specific molecular system, Fukui function was calculated using electron density of three states, shown in eqs 6−8

$$f^+(r) = \rho_{N+1}(r) - \rho_N(r) \approx \rho^{LUMO}(r) \quad (6)$$

$$f^-(r) = \rho_N(r) - \rho_{N-1}(r) \approx \rho^{HOMO}(r) \quad (7)$$

$$f^0(r) = \frac{f^+(r) + f^-(r)}{2} = \frac{\rho_{N+1}(r) - \rho_{N-1}(r)}{2} \approx \frac{\rho^{HOMO}(r) + \rho^{LUMO}(r)}{2} \quad (8)$$

In the above formula, N means the number of electrons in the current molecular system. The $N-1$ and $N+1$ states share the same molecular geometry as the N state. f^- stands for the reactivity descriptor of nucleophiles and f^+ stands for the descriptor of electrophiles. f^0 is reactivity descriptor for radical attack. Atoms with larger Fukui function would have higher reactivities. Molecular electrostatic potentials (MEPs) were also plotted via VMD 1.9.3 program.[36] DFT calculations were supported by high performance center at Shanghai Jiao Tong University.

RESULTS AND DISCUSSION

Analysis of Sol Fraction in Reclaimed SBR Under Different Conditions. After swollen with 200 phr of soybean oil, the vulcanized SBR blended with 5 phr of H_2O_2 was treated under different atmosphere at 100 °C. The samples without H_2O_2 and under nitrogen atmosphere were used as the control. Our previous study showed that 200 phr of soybean oil can sufficiently swell the rubber networks and allow effective penetration of oxygen.[24] The sol fraction indicates the breakdown extent of rubber chain scission. The sol fraction of the reclaimed samples containing H_2O_2 was significantly increased under an air atmosphere as compared to that without H_2O_2 under a N_2 atmosphere, as shown in Figure 1. The highest

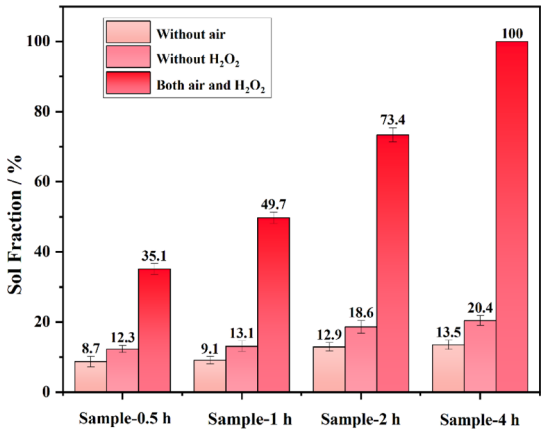


Figure 1. Effect of reaction time and addition of H_2O_2 on the reclamation efficiency of vulcanized SBR.

sol fraction reached 100% for the sample containing 5 phr of H_2O_2. The cross-linked SBR network was sufficiently swollen by soybean oil, which allows the H_2O_2 and oxygen to penetrate into the rubber network. In comparison, the reclamation without H_2O_2 had a sol fraction increase by 79.6%.[24]

The main objective of this study is to clarify the mechanism of H_2O_2-induced thermo-oxidative reclamation. 200 phr of soybean oil was used to effectively swell the rubber matrix and facilitate the penetration of H_2O_2 into the rubber structures. In addition, we tried to reduce the cost by balancing the sol of the reclaimed samples, soybean oil content, and the reclaiming temperature. The results are shown in Table S2. The results showed that less soybean content still works to hinder the re-crosslinking reactions during the reclamation of the vulcanized SBR.

Vulcanized SBR underwent a slow thermo-oxidation process at 100 °C, following an auto-oxidation process, that is, initiation, propagation, and termination.[37] The initiation generates various macroradicals and accumulation of hydroperoxides, which is a rate-determining step. H_2O_2 thermally decomposes into hydroxyl radical (•OH), which can induce auto-oxidation of the rubber and accelerate the accumulation of hydroperoxides, therefore, highly improving the reclaiming efficiency.

Analysis of Molecular Weight of the Sol and Horikx's Theory. The weight-average molecular weight (M_w) of the sol and cross-link density of the reclaimed samples after the treatment of gradient concentrations of H_2O_2 are shown in Table 1. With the increasing dose of H_2O_2, the molecular weight of the sol decreased as well as the cross-link density of the gel. With 5 phr of H_2O_2, the cross-link density of the reclaimed samples slightly declined at 0.5 h compared with the untreated samples because of the slow initiation reaction of thermo-oxidation. After 4 h, the network of vulcanized SBR was completely broken down. The decrease of M_w of the sol fraction is due to chain scission.

https://dx.doi.org/10.1021/acssuschemeng.0c08867
ACS Sustainable Chem. Eng. XXXX, XXX, XXX−XXX

Table 1. M_w of the Sol Fraction and the Value of Cross-link Density of the Reclaimed Samples

samples	cross-link density ($\times 10^{-4}$ mol/cm^3)	M_w ($\times 10^4$ g/mol)
$RSBR_{200}$-4	0.35	3.425
RH_1SBR_{200}-4	0.32	3.198
RH_2SBR_{200}-4	0.25	2.715
RH_3SBR_{200}-4	0.18	2.163
RH_4SBR_{200}-4	0.10	1.845
RH_5SBR_{200}-0.5	0.63	5.963
RH_5SBR_{200}-1	0.46	4.738
RH_5SBR_{200}-2	0.35	3.257
RH_5SBR_{200}-4		1.378
SBR	0.73	7.642

To understand the scission section in the main chain or cross-links during the reclamation process, Horikx explained the differences of two forms of chain scissions by comparing the value of sol fraction and the decline of cross-link density.[38] The solid line in Figure 2 stands for the main chain scission only, and the dashed line represents scission of cross-links only. In the latter case, sol only forms until all the cross-links are broken down, so that the polymer chains can be extracted from the rubber matrix.

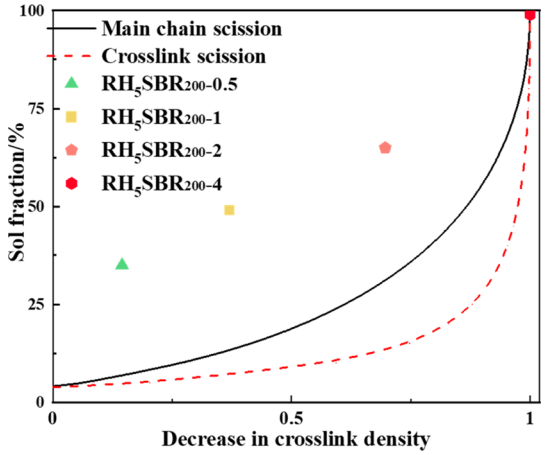


Figure 2. Horikx's plot of the data from the reclaimed samples of the vulcanized SBR for different durations.

As shown in Figure 2, all the data points are located above the solid line. This indicates that reclamation of SBR mainly took place in the main chains according to Horikx's theory. The cross-link density decreased to zero until the H_2O_2 increased to 5 phr. The data for the reclaimed samples reached the vertex point of the two lines, suggesting that the chain scission reaction dominated as the degradation duration was prolonged. At this stage, the SBR network was completely destroyed and the samples became soluble. In our previous study on SBR reclamation,[24] all points were also distributed above the solid line, suggesting that the degradation was mainly dominated by main chain scissions. However, a longer reaction period led to a back turn of points to the left side and increased the cross-link density, indicating a re-crosslinking reaction during the reclamation process. From the results mentioned above, H_2O_2 decomposed into oxidative free radical and suppressed the re-crosslinking reaction during the reclamation of SBR.

Structure Monitoring before and after Reclamation. The structure of the vulcanized SBR before and after reclamation was analyzed with ATR−FTIR spectroscopy. To facilitate the discussion, the whole spectrum was separated into three parts as shown in Figure 3.[39] The absorptions at 1650−1800 and 3300−3650 cm^{-1} were assigned to carbonyl and hydroxyl groups, respectively.[40] New peaks at 1091 and 1157 cm^{-1} were assigned to S−O bonds and C−O bonds, respectively.

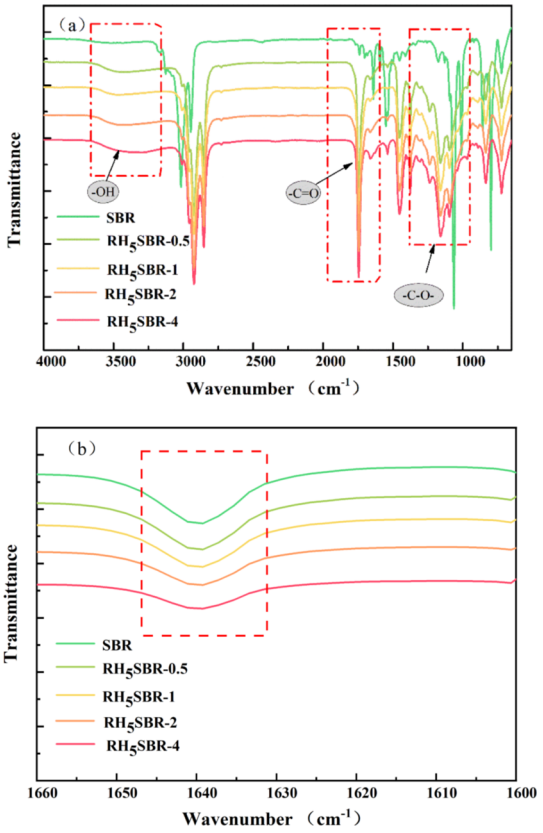


Figure 3. ATR−FTIR spectra of SBR and of RHSBRs: (a) SBR and (b) reclaimed SBR.

After reclamation at 100 °C for 0.5 h, new absorption peaks were found ranging between 1650−1800 and 3300−3650 cm^{-1}; meanwhile, the peak intensity of C−O rapidly increased over time. In addition, the intensity of peaks at the ranges of 1000 and 1300 cm^{-1} also increased, suggesting the generation of C−O bonds in the form of alcohols, ethers, or esters. The peak intensity of −C═CH at 1640 cm^{-1} decreased over time, which indicated that the −C═CH group was also attacked. The characteristic peaks of benzene groups remained almost unchanged in the region of 1450−1650 cm^{-1}. This might be attributed to the fact that the aliphatic groups were more easily oxidized than the aromatic groups in the SBR polymer chains.

The chain scission of SBR occurred during oxidative reclamation at 100 °C, resulting in liquid reclaimed rubber. This was distinguished from the traditional oxidation of rubber at low temperature. As shown in Figure 4, the ^{13}C NMR spectra of SBR and reclaimed SBR were compared. New resonance at δ = 68.7, δ = 125−135, and δ = 172.9 ppm is observed compared to that of SBR.[41] The results from ATR−FTIR and NMR demonstrated that thermo-oxidative reaction of SBR contains complex reactions related to oxygenated chemicals such as alcohol, ketone, and carboxylic acid species.

https://dx.doi.org/10.1021/acssuschemeng.0c08867
ACS Sustainable Chem. Eng. XXXX, XXX, XXX−XXX

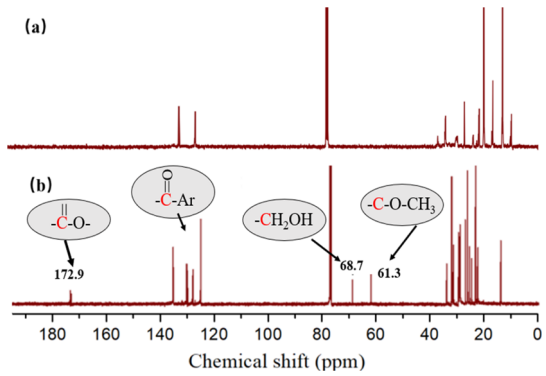


Figure 4. ^{13}C NMR of the samples: (a) SBR and (b) reclaimed SBR.

The molecular weight of SBR significantly decreased as a result of chain scission during the reclamation. This may be attributed to the oxidative reaction of the polymer main chains of SBR attacked by the hydroxyl radicals from the decomposition of H_2O_2.

Oxidative Reclamation Mechanism of Vulcanized SBR Induced by H_2O_2. Fukui function is a powerful tool to explore reactivity and site selectivity.[42] By calculating Fukui functions, we will be able to determine the active sites of ordinary rubber and SBR, based on the electronic density. To understand the reaction pathway of SBR reclamation at the molecular level, Fukui function analysis was undertaken based on the previous optimized structures. Monomer species were built as a model system. For simplification, styrene and 1-butene were chosen to represent ordinary rubber and SBR, respectively, calculating which to obtain the reaction site prediction.

First, we explored which functional groups in SBR are easily attacked, as well as identified where the atoms in 1-butene are more positive, and the most active site of hydrogen atom was located in the methylene group of 1-butene. By decomposing Fukui function as atom contributions, we further obtained the quantitative indicator of contribution of atoms to the total Fukui function index. As shown in Tables 2 and 3, H7 atom shows the

Table 2. Comparison of the Values of Hirshfeld Charges and Fukui Functions for Each Hydrogen Atom in Cumene

atom	Q(N)	q($N+1$)	q($N-1$)	F0
10 (H)	0.0291	0.0085	0.0515	0.0215
11 (H)	0.0282	0.0174	0.0430	0.0128
12 (H)	0.0291	−0.0021	0.0639	0.0330
13 (H)	0.0309	0.0180	0.0473	0.0147
14 (H)	0.0309	0.0180	0.0473	0.0147
15 (H)	0.0291	−0.0021	0.0639	0.0330
16 (H)	0.0282	0.0174	0.0430	0.0128
17 (H)	0.0380	−0.0026	0.0807	0.0416
18 (H)	0.0386	−0.0176	0.0795	0.0486
19 (H)	0.0422	−0.0204	0.0877	0.0541
20 (H)	0.0420	−0.0018	0.00854	0.0436
21 (H)	0.0421	−0.0152	0.0976	0.0564

biggest values of Fukui functions in 1-butene, which is located in the methylene group, as shown in Figure 5a,b. Compared with the values of Fukui functions of 1-butene, the values of hydrogen atoms in cumene are much smaller, so the volume displayed on the isosurface is smaller than that of 1-butene.

Molecular electrostatic potential (MESP) is useful in investigating the molecular physicochemical properties, along

Table 3. Comparison of the Values of Hirshfeld Charges and Fukui Functions for Each Hydrogen Atom in 1-Butene

atom	q(N)	q($N+1$)	q($N-1$)	F0
2 (H)	0.0325	−0.0326	0.1029	0.0677
3 (H)	0.0378	−0.0385	0.1069	0.0727
6 (H)	0.0378	−0.0385	0.0169	0.0727
7 (H)	0.0377	−0.0509	0.1185	0.0847
8 (H)	0..0357	−0.0492	0.1134	0.0813
10 (H)	0.0305	−0.0483	0.0790	0.0637
11(H)	0.0293	−0.0027	0.0587	0.0307
12 (H)	0.0301	−0.0009	0.0592	0.0300

with the charge distributions in molecules in terms of color grading. The most negative site is the preferred region for electrophilic attack and is indicated in blue. The red parts represented the positive region, which is preferable for nucleophilic attack.[43] We also calculated the MESP of cumene and 1-butene. As shown in Figure 5c,d, the most positive electrostatic potential comes up on the methylene group of 1-butene, which means that the methylene group is liable to electrophilic attack.

DFT calculation further suggested that the hydroxyl radical that resulted from the thermal cracking cleavage of hydrogen peroxide can react with SBR, which could be an additional pathway for the oxidation of SBR. Hydroxyl radical reacts with the aliphatic part of SBR during the reaction process. Hydrogen peroxide would undergo homolytic cleavage and form the hydroxyl radicals. The corresponding bond dissociation energy (BDE) was 52.5 kcal/mol. The hydroxyl radical can further react with the aliphatic part of SBR. The corresponding potential energy surface (PES) of the reaction system is depicted in Figure 6.

In the process of hydrogen abstraction reactions, the hydroxyl radical may capture the hydrogen atoms from the methylene group of SBR, forming a water molecule and intermediate IM1 with the corresponding energy barrier of 4.7 kcal/mol. Interestingly, the H7 atom connected to C═C bond in 1-butene was easier to release with lower energy barrier (4.7 kcal/mol) than that (8.1 kcal/mol) of the H10 atom (Figure 6a,b). Hydrogen abstraction reaction of cumene was favorable at the aromatic ring, in which the hydrogen atom showed a larger value of $f0$(Fukui function) than that located on the main chain, indicating that it was easier to be attacked by $^{\bullet}OH$. When alkyl radicals $R^{\bullet}$ were generated, it would react with molecular oxygen through barrierless addition, forming alkyl hydroperoxides $ROO^{\bullet}$ radical. As seen from Figure 6c, the plot of the potential energy curve would monotonically decrease as the O_2 molecule approached $R^{\bullet}$ until the formation of the radical intermediate $ROO^{\bullet}$. The PES change along the variation of the C−O distance showed that no TS exists on the $R^{\bullet} + O_2$ reaction process.

As alkyl hydroperoxides $ROO^{\bullet}$ are generated, the peroxyl radicals then propagate to the oxidative chain. The reaction mechanism can be concluded as $ROO^{\bullet} + RH \rightarrow ROOH + R^{\bullet}$, as shown in Figure 6b. Alkyl hydroperoxides ($ROO^{\bullet}$) radical would further attack RH, which induced the formation of ROOH and $R^{\bullet}$ with a corresponding energy barrier and the Gibbs free energy changes (ΔG^{θ}) of 5.9 kcal/mol and −19.0, respectively. In order to verify the degradation mechanism of vulcanized SBR proposed above, we compared the chemical mechanism developed using DFT method with the other mechanism in the existing literature. The detailed analysis is shown in the Supporting Information.

https://dx.doi.org/10.1021/acssuschemeng.0c08867
ACS Sustainable Chem. Eng. XXXX, XXX, XXX−XXX

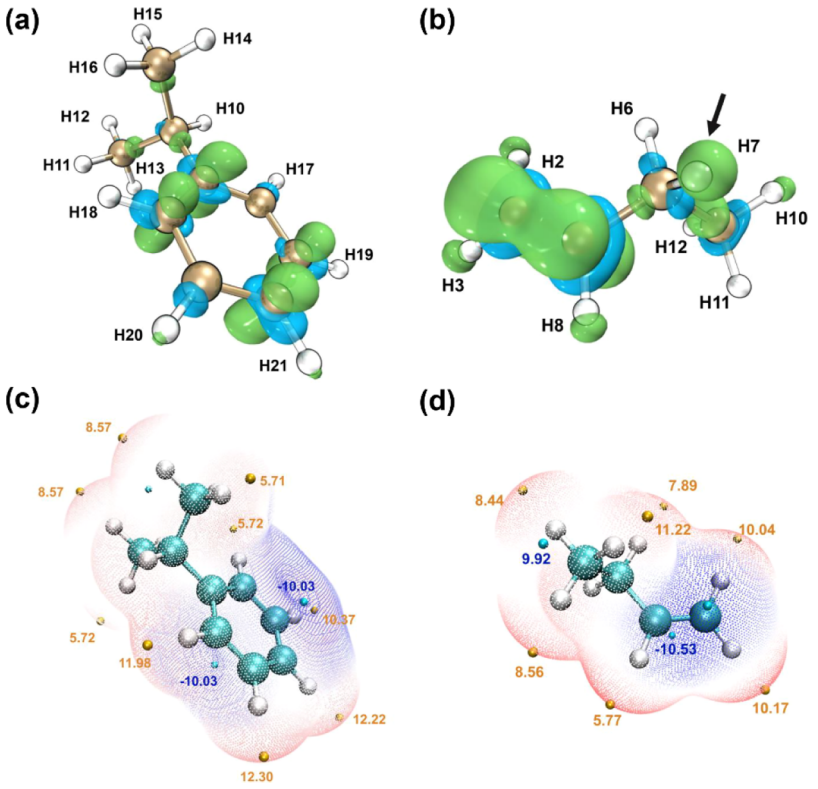


Figure 5. Reaction site prediction via Fukui function analysis and MESP analysis. Fukui function plots ($f0$) (isosurface value = ±0.007) for cumene (a) and 1-butene (b). Green and blue isosurfaces represent positive and negative parts, respectively. The MESP plots of the reactant were computed for the model of SBR (c) and ordinary rubber (d) for simplification.

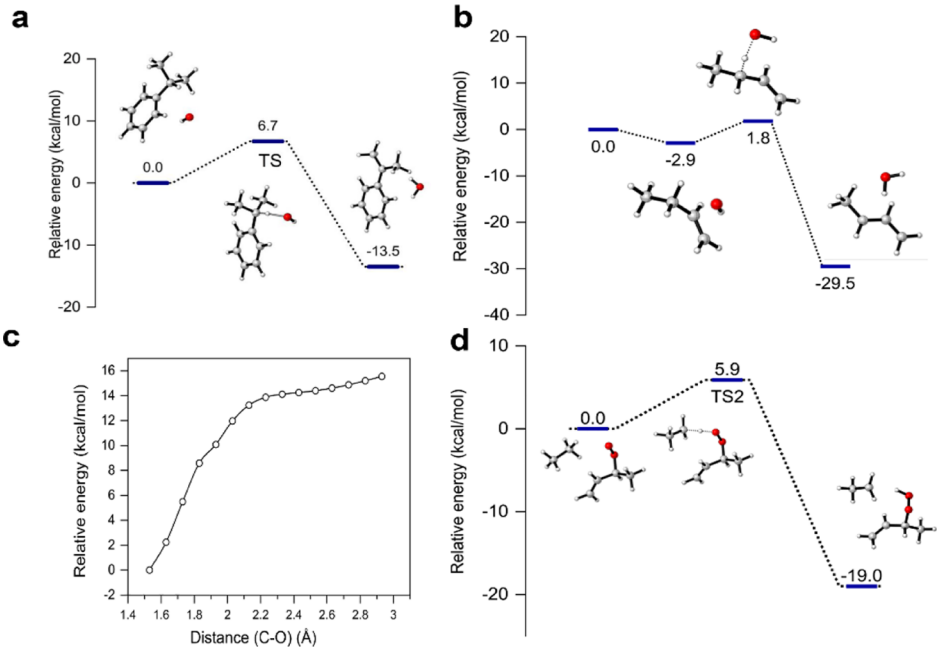


Figure 6. Potential profiles along the reaction pathways and corresponding TS for the possible pathway of SBR. (a) Pathway of hydrogen abstraction reactions between cumene and $^{\bullet}$OH. (b) Reaction of hydrogen abstraction reactions between 1-butene and $^{\bullet}$OH. (c) DFT calculation of potential energy profiles of intermediate alkyl radical R$^{\bullet}$−O_2 dissociation at M06-2X/6-311+G(d,p) level of theory. (d) Pathway from alkyl hydroperoxides (ROO$^{\bullet}$) radical to ROOH product.

Based on the results of theoretical calculation, a possible reclamation mechanism of vulcanized SBR is shown in Figure 7.

Model-Free Kinetics Analysis. A kinetic analysis of the reclamation process is very important to understand the reclamation mechanism by calculating the kinetics model and parameters based on thermogravimetric data.[29] The reaction routines and mechanism are mainly determined by the activation energy (E_a).

https://dx.doi.org/10.1021/acssuschemeng.0c08867
ACS Sustainable Chem. Eng. XXXX, XXX, XXX−XXX

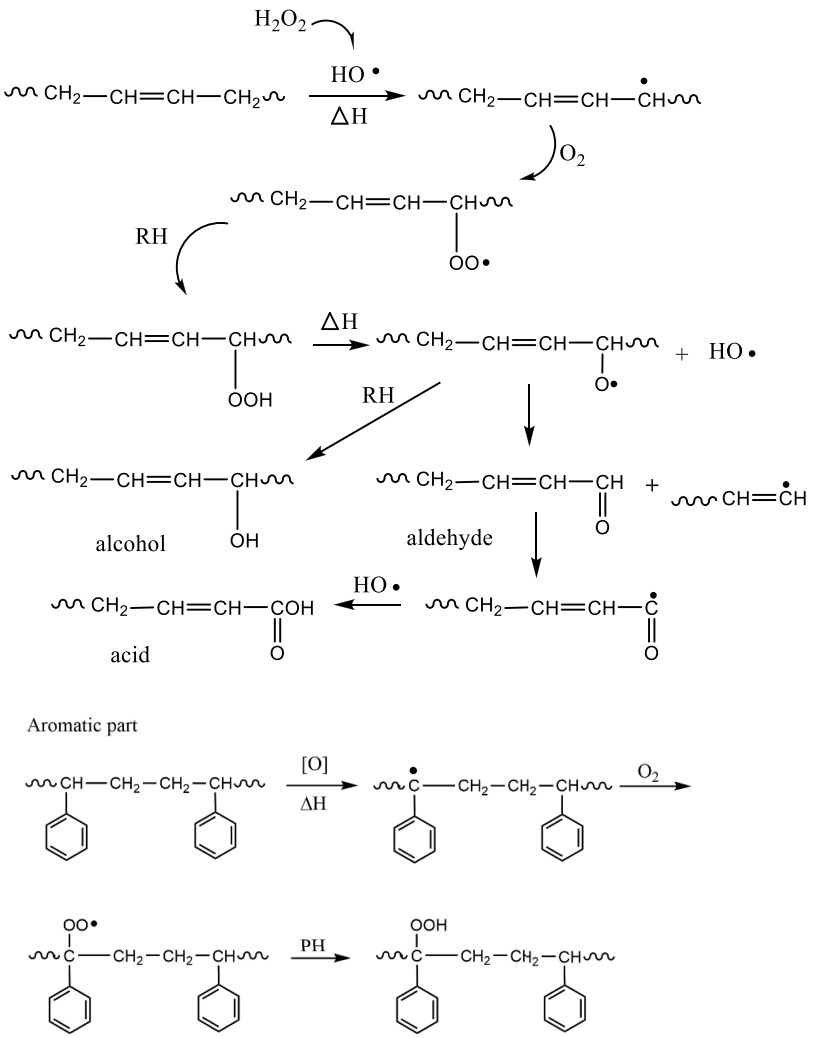


Figure 7. Schematic reaction of oxidative reclamation process (R• represents macromolecular radicals).

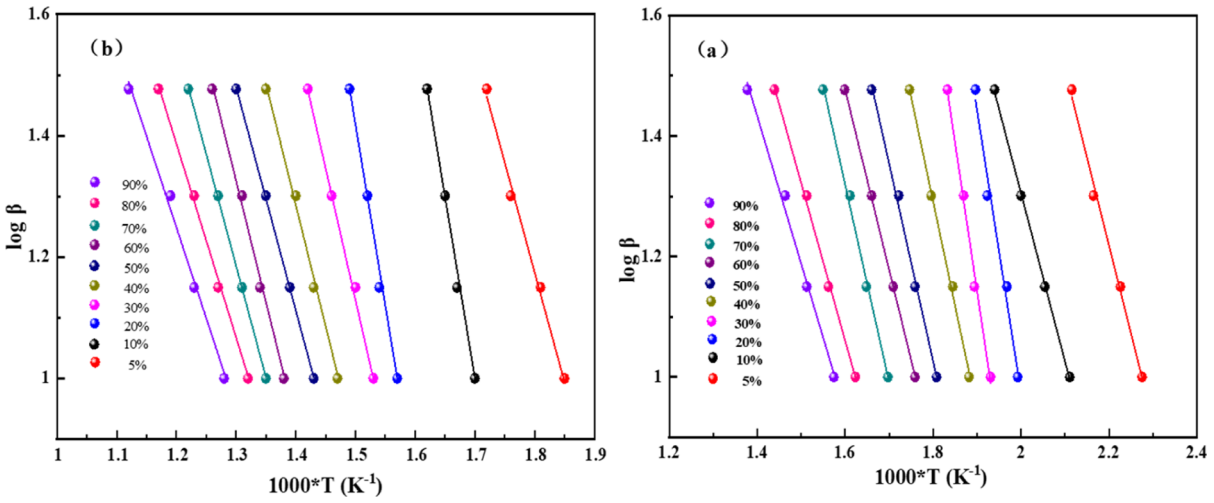


Figure 8. Linear fitting result of SBR using FWO method. (a) Vulcanized SBR and (b) Vulcanized SBR with the addition of H_2O_2.

Figure 8 showed linear fittings according to the weight loss data obtained at different heating rates to solve the value of E_a. The values of E_a can be obtained corresponding to the conversion degrees from 0.05 to 0.90, as shown in Figure 9. The relationship of E_a versus reclamation conversion was shown. It was obvious that the value of E_a did not remain unchanged but decreased with reclamation conversion. The maximum value of E_a appeared at the initial stage. That means that the thermo-oxidation of SBR was not a one-step reaction but followed a complex multiple step mechanism. In addition, E_a existing in other literature was compared with the above value, and the

https://dx.doi.org/10.1021/acssuschemeng.0c08867
ACS Sustainable Chem. Eng. XXXX, XXX, XXX−XXX

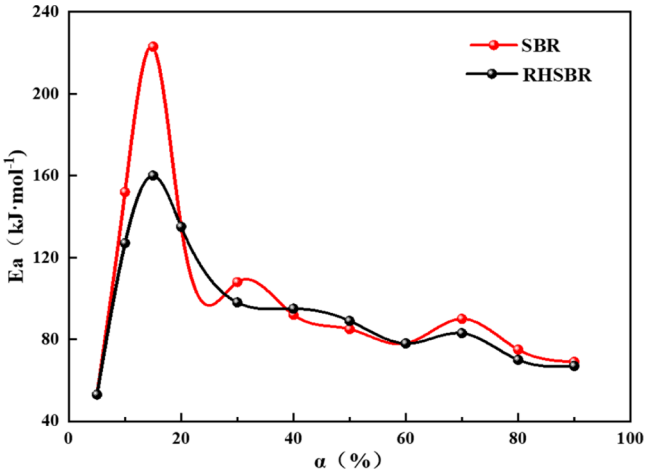


Figure 9. Relationship of activation energy versus thermo-oxidative conversion.

results are shown in Table S1. The model-free method is thus suitable for kinetics analysis of SBR.

Based on the above analysis, the thermo-oxidative reclamation process consists of three stages: (1) Initiation of free macroradicals: At the initial stage of thermo-oxidative reclamation, allylic radicals are easily generated because of high reactivity of α-H in the main chains. Double bonds in the polymer main chains are also easily attacked. Moreover, the formation of allylic macroradicals dominates the thermo-oxidative reclamation along with a small proportion of other alkyl free macroradicals. The formation of a variety of free radicals takes place during the whole thermo-oxidation reclamation. (2) Initial oxidation process: Because of the presence of oxygen in air, these free allylic radicals are easily oxidized to form hydroperoxide. These primary hydroperoxide species decompose rapidly into carbonyl groups until its concentration has accumulated to a relatively low value. During this stage, there are numerous highly reactive allylic radicals accumulated in the polymer. (3) Deep oxidation stage: A large number of hydrogen atoms are extracted from the main chains of SBR polymer and then the formation of alkyl radicals or hydroperoxides occurs during this reclamation stage. Subsequently, the reclamation products containing carboxyl, hydroxyl, and aldehyde groups, and so on were generated. According to the model-free kinetics results, E_a of the initial stage in the oxidative reclamation process decreased from 223 to 160 kJ/mol by the addition of H_2O_2. This indicates that the addition of H_2O_2 may induce the autocatalytic reactions and accelerate the thermo-oxidation of SBR.

CONCLUSIONS

The recycling of vulcanized SBR often involves re-crosslinking reactions which hinders the reclamation efficiency of waste tire rubber. In this work, the vulcanized SBR was transformed into reclaimed rubber with 100% sol fraction by a H_2O_2-induced oxidative reclamation process at 100 °C. This process overcomes the re-crosslinking reaction during the reclamation of SBR without the need of using sulfur-containing chemical agents and high temperature.

The vulcanized SBR underwent a severe oxidative scission and was then transformed into highly reclaimed rubber. Various functional groups, such as carboxyl and hydroxyl groups, were generated on the polymer chains. Moreover, the reaction pathway of oxidative reclamation was inferred through DFT calculations. It showed that the hydroxyl radical resulting from homolytic cleavage reaction of H_2O_2 can react with SBR via hydrogen abstraction reaction, which greatly accelerates the rate-determining step of the SBR oxidation. The apparent activation energy (E_a) of the initial stage in the H_2O_2-induced oxidative reclamation process decreased from 223 to 160 kJ/mol.

Compared with the traditional chemical reclaiming methods, this study provides an effective and eco-friendly method for reclaiming SBR. Although much oil was employed to reclaim the SBR vulcanizates, the reclaimed rubber with reactive functional groups will open up new applications for recycled rubber products.

ASSOCIATED CONTENT

Supporting Information

The Supporting Information is available free of charge at https://pubs.acs.org/doi/10.1021/acssuschemeng.0c08867.

Comparison of chemical mechanism developed by DFT with other existing mechanism in the literature, comparison of E_a with other existing literature, and effects of less oil content and higher temperature on the reclamation of the vulcanized SBR (PDF)

AUTHOR INFORMATION

Corresponding Author

Shifeng Wang − *Department of Polymer Science and Engineering, Shanghai Jiao Tong University, Shanghai 200240, China;* orcid.org/0000-0003-0050-8077; Email: shfwang@sjtu.edu.cn

Authors

Zhen Zhang − *Department of Polymer Science and Engineering, Shanghai Jiao Tong University, Shanghai 200240, China*

Jiayi Li − *State Key Laboratory of Microbial Metabolism, Joint International Research Laboratory of Metabolic and Developmental Sciences, School of Life Sciences and Biotechnology, Shanghai Jiao Tong University, Shanghai 200240, China*

Chaoying Wan − *International Institute for Nanocomposites Manufacturing (IINM), University of Warwick, Coventry CV4 7AL, U.K.;* orcid.org/0000-0002-1079-5885

Yuxin Zhang − *Department of Polymer Science and Engineering, Shanghai Jiao Tong University, Shanghai 200240, China*

Complete contact information is available at: https://pubs.acs.org/10.1021/acssuschemeng.0c08867

Notes

The authors declare no competing financial interest.

ACKNOWLEDGMENTS

The authors are grateful for the research foundation provided by International Cooperation Project by MOST, SQ2019YFE012146, Natural Science Foundation of China (no. 51273110), and the Jiangsu Science and Technology Project (BA2016002).

REFERENCES

(1) Thomas, B. S.; Gupta, R. C. A comprehensive review on the applications of waste tire rubber in cement concrete. *Renew. Sustain. Energy Rev.* **2016**, *54*, 1323−1333.

https://dx.doi.org/10.1021/acssuschemeng.0c08867
ACS Sustainable Chem. Eng. XXXX, XXX, XXX−XXX

(2) Mohajerani, A.; Burnett, L.; Smith, J. V.; Markovski, S.; Rodwell, G.; Rahman, M. T.; Kurmus, H.; Mirzababaei, M.; Arulrajah, A.; Horpibulsuk, S.; Maghool, F. Recycling waste rubber tyres in construction materials and associated environmental considerations: A review. *Resour. Conserv. Recycl.* **2020**, *155*, 104679−104696.
(3) Sienkiewicz, M.; Janik, H.; Borzędowska-Labuda, K.; Kucińska-Lipka, J. Environmentally friendly polymer-rubber composites obtained from waste tyres: A review. *J. Clean. Prod.* **2017**, *147*, 560−571.
(4) Myhre, M.; Saiwari, S.; Dierkes, W. K.; Noordermeer, J. Rubber Recycling: Chemistry, Processing, and Applications. *Rubber Chem. Technol.* **2012**, *85*, 408−449.
(5) Bockstal, L.; Berchem, T.; Schmetz, Q.; Richel, A. Devulcanisation and reclaiming of tires and rubber by physical and chemical processes: A review. *J. Clean. Prod.* **2019**, *236*, 117574−117590.
(6) Aoudia, K.; Azem, S.; Aït Hocine, N.; Gratton, M.; Pettarin, V.; Seghar, S. Recycling of waste tire rubber: Microwave devulcanization and incorporation in a thermoset resin. *Waste Manag.* **2017**, *60*, 471−481.
(7) Asaro, L.; Gratton, M.; Seghar, S.; Aït Hocine, N. Recycling of rubber wastes by devulcanization. *Resour. Conserv. Recycl.* **2018**, *133*, 250−262.
(8) Martínez, J. D.; Puy, N.; Murillo, R.; García, T.; Navarro, M. V.; Mastral, A. M. Waste tyre pyrolysis−A review. *Renew. Sustain. Energy Rev.* **2013**, *23*, 179−213.
(9) Cheng, X.; Song, P.; Zhao, X.; Peng, Z.; Wang, S. Liquefaction of ground tire rubber at low temperature. *Waste Manag.* **2018**, *71*, 301−310.
(10) Zhang, Y.; Zhang, Z.; Wemyss, A. M.; Wan, C.; Liu, Y.; Song, P.; Wang, S. Effective Thermal-Oxidative Reclamation of Waste Tire Rubbers for Producing High-Performance Rubber Composites. *ACS Sustain. Chem. Eng.* **2020**, *8*, 9079−9087.
(11) Shi, J.; Zou, H.; Ding, L.; Li, X.; Jiang, K.; Chen, T.; Zhang, X.; Zhang, L.; Ren, D. Continuous production of liquid reclaimed rubber from ground tire rubber and its application as reactive polymeric plasticizer. *Polym. Degrad. Stab.* **2014**, *99*, 166−175.
(12) Shi, J.; Jiang, K.; Ren, D.; Zou, H.; Wang, Y.; Lv, X.; Zhang, L. Structure and performance of reclaimed rubber obtained by different methods. *J. Appl. Polym. Sci.* **2013**, *129*, 999−1007.
(13) Danielle Galiani, P.; Antonio Malmonge, J.; Guenther Soares, B.; Henrique Capparelli Mattoso, L. Studies on thermal−oxidative degradation behaviours of raw natural rubber: PRI and thermogravimetry analysis. *Plast., Rubber Compos.* **2013**, *42*, 334−339.
(14) Xiang, K.; Wang, X.; Huang, G.; Zheng, J.; Huang, J.; Li, G. Thermal ageing behavior of styrene−butadiene random copolymer: A study on the ageing mechanism and relaxation properties. *Polym. Degrad. Stab.* **2012**, *97*, 1704−1715.
(15) Vernáez, O.; Dagreou, S.; Grassl, B.; Müller, A. J. Degradation of styrene butadiene rubber (SBR) in anaerobic conditions. *Polym. Degrad. Stab.* **2015**, *111*, 159−168.
(16) Saiwari, S.; Dierkes, W. K.; Noordermeer, J. Devulcanization of Whole Passenger Car Tire Material. *kgk-rubberpoint* **2013**, *66*, 20−25. http://purl.utwente.nl/publications/88392
(17) Levin, V. Y.; Kim, S. H.; Isayev, A. I. Effect of Crosslink Type on the Ultrasound Devulcanization of SBR Vulcanizates. *Rubber Chem. Technol.* **1997**, *70*, 641−649.
(18) Hong, C. K.; Isayev, A. I. Continuous ultrasonic devulcanization of NR/SBR blends. *J. Appl. Polym. Sci.* **2002**, *83*, 160−168.
(19) Mangili, I.; Lasagni, M.; Huang, K.; Isayev, A. I. Modeling and optimization of ultrasonic devulcanization using the response surface methodology based on central composite face-centered design. *Chemometr. Intell. Lab. Syst.* **2015**, *144*, 1−10.
(20) Isayev, A. I., Recycling of natural and synthetic isoprene rubbers. *Chemistry, Manufacture and Applications of Natural Rubber*; Woodhead Publishing Limited, 2014; pp 395−435. DOI: 10.1533/9780857096913.3.395
(21) Guo, L.; Huang, G.; Zheng, J.; Li, G. Thermal oxidative degradation of styrene-butadiene rubber (SBR) studied by 2D correlation analysis and kinetic analysis. *J. Therm. Anal. Calorim.* **2013**, *115*, 647−657.
(22) Rasool, R. t.; Song, P.; Wang, S. Thermal analysis on the interactions among asphalt modified with SBS and different degraded tire rubber. *Constr. Build. Mater.* **2018**, *182*, 134−143.
(23) Saiwari, S.; Noordermeer, J. W. M.; Dierkes, W. K. Comparative Investigation of the Devulcanization Parameters of Tire Rubbers. *Rubber Chem. Technol.* **2014**, *87*, 31−42.
(24) Zhang, Z.; Wan, C.; Song, P.; Xie, Y.; Zhang, Y.; Wang, S. Soybean oil induced efficient thermal−oxidative degradation of covalently crosslinked styrene butadiene rubber. *J. Appl. Polym. Sci.* **2019**, *137*, 48935−48946.
(25) Córdoba, A.; Saux, C.; Pierella, L. B. Kinetic Modelling of the catalytic oxidation of 2-(methylmercapto)-benzothiazole under mild conditions. *Appl. Catal., A* **2017**, *544*, 173−180.
(26) Bokare, A. D.; Choi, W. Review of iron-free Fenton-like systems for activating H2O2 in advanced oxidation processes. *J. Hazard. Mater.* **2014**, *275*, 121−135.
(27) Ibrahim, S.; Daik, R.; Abdullah, I. Functionalization of Liquid Natural Rubber via Oxidative Degradation of Natural Rubber. *Polymers* **2014**, *6*, 2928−2941.
(28) Liu, S.; Yu, J.; Bikane, K.; Chen, T.; Ma, C.; Wang, B.; Sun, L. Rubber pyrolysis: Kinetic modeling and vulcanization effects. *Energy* **2018**, *155*, 215−225.
(29) Danon, B.; Mkhize, N. M.; van der Gryp, P.; Görgens, J. F. Combined model-free and model-based devolatilisation kinetics of tyre rubbers. *Thermochimi. Acta* **2015**, *601*, 45−53.
(30) Zheng, W.; Jia, Z.; Zhang, Z.; Yang, W.; Zhang, L.; Wu, S. Improvements of lanthanum complex on the thermal-oxidative stability of natural rubber. *J. Mater. Sci.* **2016**, *51*, 9043−9056.
(31) Zhao, Y.; Truhlar, D. G. The M06 suite of density functionals for main group thermochemistry, thermochemical kinetics, noncovalent interactions, excited states, and transition elements: two new functionals and systematic testing of four M06-class functionals and 12 other functionals. *Theor. Chem. Acc.* **2007**, *120*, 215−241.
(32) Frisch, M. J.; Trucks, G. W.; Schlegel, H. B.; Scuseria, G. E.; Robb, M. A.; Cheeseman, J. R.; Scalmani, G.; Barone, V.; Petersson, G. A.; Nakatsuji, H.; Li, X.; Caricato, M.; Marenich, A. V.; Bloino, J.; Janesko, B. G.; Gomperts, R.; Mennucci, B.; Hratchian, H. P.; Ortiz, J. V.; Izmaylov, A. F.; Sonnenberg, J. L.; Williams; Ding, F.; Lipparini, F.; Egidi, F.; Goings, J.; Peng, B.; Petrone, A.; Henderson, T.; Ranasinghe, D.; Zakrzewski, V. G.; Gao, J.; Rega, N.; Zheng, G.; Liang, W.; Hada, M.; Ehara, M.; Toyota, K.; Fukuda, R.; Hasegawa, J.; Ishida, M.; Nakajima, T.; Honda, Y.; Kitao, O.; Nakai, H.; Vreven, T.; Throssell, K.; Montgomery, Jr., J. A.; Peralta, J. E.; Ogliaro, F.; Bearpark, M. J.; Heyd, J. J.; Brothers, E. N.; Kudin, K. N.; Staroverov, V. N.; Keith, T. A.; Kobayashi, R.; Normand, J.; Raghavachari, K.; Rendell, A. P.; Burant, J. C.; Iyengar, S. S.; Tomasi, J.; Cossi, M.; Millam, J. M.; Klene, M.; Adamo, C.; Cammi, R.; Ochterski, J. W.; Martin, R. L.; Morokuma, K.; Farkas, O.; Foresman, J. B.; Fox, D. J. *Gaussian 16*, Revision B.01; Wallingford, CT, 2016.
(33) Lu, T.; Chen, F. Multiwfn: a multifunctional wavefunction analyzer. *J. Comput. Chem.* **2012**, *33*, 580−592.
(34) Parr, R. G.; Yang, W. Density Functional Approach to the Frontier-Electron Theory of Chemical Reactivity. *J. Am. Chem. Soc.* **1984**, *106*, 4049−4050.
(35) Fukui, K.; Yonezawa, T.; Shingu, H. A Molecular Orbital Theory of Reactivity in Aromatic Hydrocarbons. *J. Chem. Phys.* **1952**, *20*, 722−725.
(36) Humphrey, W.; Dalke, A.; Schulten, K. VMD: Visual Molecular Dynamics. *J. Mol. Graph.* **1996**, *14*, 33−38.
(37) Munteanu, S. B.; Brebu, M.; Vasile, C. Thermal and thermo-oxidative behaviour of butadiene−styrene copolymers with different architectures. *Polym. Degrad. Stab.* **2005**, *89*, 501−512.
(38) Horikx, M. M. Chain Scissions in a Polymer Network. *J. Polym. Sci.* **1956**, *19*, 445−454.
(39) Colom, X.; Faliq, A.; Formela, K.; Cañavate, J. FTIR spectroscopic and thermogravimetric characterization of ground tyre rubber devulcanized by microwave treatment. *Polym. Test.* **2016**, *52*, 200−208.

https://dx.doi.org/10.1021/acssuschemeng.0c08867
ACS Sustainable Chem. Eng. XXXX, XXX, XXX−XXX

(40) Zhi, J.; Wang, Q.; Zhang, M.; Zhou, Z.; Liu, A.; Jia, Y. Coupled analysis on hyper-viscoelastic mechanical behavior and macromolecular network alteration of rubber during thermo-oxidative aging process. *Polymer* **2019**, *171*, 15−24.
(41) Arantes, T. M.; Leão, K. V.; Tavares, M. I. B.; Ferreira, A. G.; Longo, E.; Camargo, E. R. NMR study of styrene-butadiene rubber (SBR) and TiO2 nanocomposites. *Polym. Test.* **2009**, *28*, 490−494.
(42) Geerlings, P.; De Proft, F.; Langenaeker, W. Conceptual density functional theory. *Chem. Rev.* **2003**, *103*, 1793−1874.
(43) Liang, Y.; Li, J.; He, Y.; Jiang, Z.; Shangguan, W. Catalytic oxidation of dimethyl phthalate over titania-supported noble metal catalysts. *J. Hazard. Mater.* **2021**, *401*, 123274−123286.

https://dx.doi.org/10.1021/acssuschemeng.0c08867
ACS Sustainable Chem. Eng. XXXX, XXX, XXX−XXX